Topological models of cellular structures

1991 J. Phys. A: Math. Gen. 24 1307

(http://iopscience.iop.org/0305-4470/24/6/022)

J. Phys. A: Math. Gen. 24 (1991) 1307-1317. Printed in the UK

Topological models of cellular structures

G Le Caër

Laboratoire de Science et Génie des Matériaux Métalliques†, URA 159, Ecole des Mines, F-54042 Nancy Cedex, France

Received 22 October 1990, in final form 18 December 1990

Abstract. A method for constructing topological models of cellular structures is described. It is based on lattices with topologically unstable sites, which belong to more than z_s polygons ($z_s = 3$ in 2D), and on rules which allow removing this degeneracy. For every value of the coordination number z and for a given rule, there are $Q(z)$ stable configurations, called states. Cellular models are associated with distributions of states on the lattice sites. The distribution of cell sides as well as other characteristics such as the correlations among cells can be derived. Many models of statistical physics may be used (Ising, Potts, cellular automata). The case $z = 4$ is discussed and observed to agree with some experimental or simulation results.

1. Introduction

As emphasized by various authors (Thompson 1917, Weaire 1983, Weaire and Rivier 1984) cellular structures abound in Nature and are of interest in many scientific fields such as metallurgy (polycrystals, Meijering 1953), geology (crack networks in basalt flows, Smalley 1966), biology (eg: biological tissues, Lewis 1928) etc. They are also widely used as models, for example in order to describe the atomic-scale structure of iono-covalent glasses (Sadoc and Mosseri 1982, Marians and Burdett 1990), or to account for the large scale structure of the universe (Coles 1990).

The present paper will focus on two-dimensional (2D) space-filling random cellular structures although the method that we describe may as well be applied to 3D cellular structures. Topological characterizations of these structures almost invariably include the distribution $P(n)$ of the number n of edges of cells (called here n-cells) or the n-dependence of the mean number $m_n(1)$ of sides of the first neighbour cells of n-cells. The mean number $m_n(i)$ of sides of the ith neighbour cells ($i > 1$) of n-cells has also been investigated by computer simulation (Nakashima *et al* 1989). An important semi-empirical law, the Aboav–Weaire law (Aboav, 1970, 1980, Weaire 1974), expresses that $m_n(1)$ is linearly related to $1/n$ by

$$m_n(1) = 6 - a + (6a + \mu_2)/n \tag{1}$$

where μ_2 is the variance of the distribution of n: $\mu_2 = \langle n^2 \rangle - \langle n \rangle^2$, with $\langle n \rangle = 6$ as a consequence of Euler's relation in 2D (Weaire and Rivier 1984) and $\langle n m_n(1) \rangle = \mu_2 + 36$ (Weaire 1974). In many natural random cellular structures, the parameter a is of the order of 1.2 (Aboav 1980). In 2D, only two transformations are needed to describe the

† Associé au CNRS.

0305-4470/91/061307+11$03.50

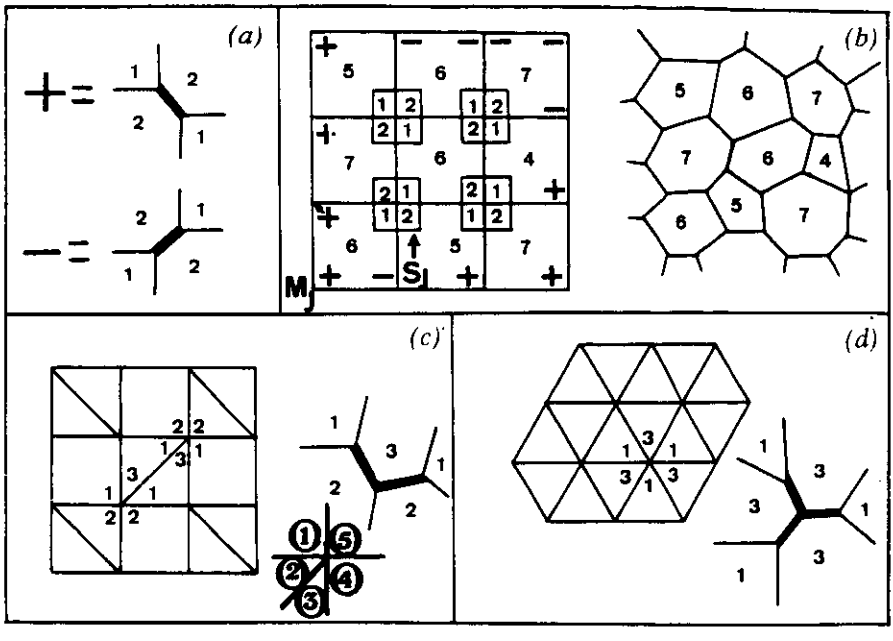

Figure 1. (*a*) The two different states for $z=4$, the associated S_{kj} ($k=+,-, j=1,\ldots,4$) values. Neighbour switching T1 is simply described here by 'spin' flipping ($+\rightarrow-$ or $-\rightarrow+$, the cells, with $S_{kj}=1$, which are not neighbours become neighbours and vice versa). (*b*) An example of a distribution of states on a square lattice, the corresponding values of the number n of cells sides and one realization of the associated cellular structure. (*c*) A lattice with $z=5$ ($a=3^2,4,3,4$ net in Schläfli notation), the numbering convention (circled numbers) and one among the five states on two different lattice sites. (*d*) A triangular lattice $z=6$ and one among the 14 states in (*a*), (*c*), (*d*) stable configurations have been drawn; bold lines represent the added cell sides.

progressive disordering of a hexagonal network. They are neighbour switching (T1, figure 1) and vanishing of cells (T2, Weaire and Rivier 1984). The Aboav-Weaire law is derived with $a=1$ when the evolution of a froth under the two previous 2D elementary structural transformations is studied, assuming no correlation beyond nearest neighbours (Blanc and Mocellin 1979, Rivier 1985). As emphasized by Weaire (1983) and Fortes and Andrade (1989), the simple linear law (1) is still not fully understood and may be not more than a good approximation.

We describe in section 2 a method which allows constructing topological models of cellular structures in which both $P(n)$ and $m_n(i)$ ($i=1,2,\ldots$) as well as other characteristics may be analytically or numerically calculated for the simplest cases and computer simulated for the more complex cases. The models are topological as they give the relative repartition of cells and does not need or give information about angles and edge lengths.

2. The method

The method, which defines a transform of a distribution of states on a lattice, is based on the following (figure 1).

(1) A lattice with topologically unstable sites. Every site is characterized by its coordination number z which is the number of edges merging in that vertex. In 2D, the vertices with $z > z_s = 3$ are structurally unstable, as their properties change by small deformations, while $z_s = 4$ in 3D. The fraction of vertices with $z_i = 3, \ldots, z$ $(z > 3)$ is f_i with $f_3 < 1$.

(2) A rule to remove the degeneracy of the unstable vertices until only $z_i = z_s$ (3 in 2D) vertices are left. This rule produces a set of $Q(z_i)$ possible stable configurations, called states.

For every state k $(k = 1, \ldots, Q(z_i))$, z_i numbers $S_{kj}(z_i)$ $(j = 1, \ldots, z_i, 1 \leqslant S_{kj} \leqslant z_i - 2)$ are specified (for example {12213} for $z_i = 5$, figure 1(*c*)) and assigned to every z_i-vertex of the lattice. They are used for calculating the number of sides n and for defining the neighbouring cells.

(3) A criterion for distributing the various states on the lattice sites. It may for example be a set of probabilities p_{ij} $(\sum_j p_{ij} = 1)$ which are used at every z_i-type site to chose among the $Q(z_i)$ possible states. Interactions among the various sites may also be defined on the starting lattice.

As we have only considered, up to now, rules which do not create or annihilate cells, we associate a cell of the topological cellular model with every polygon of the lattice, or spherical polygon (Coxeter 1973) if a spherical tessellation is considered. The topological model is deduced from the previous distribution of states. The number of cell sides n is obtained by summing up the S_{kj} values which are inside the corresponding lattice polygon (figure 1(*b*)). The method will be discussed for a square lattice ($z = 4$, $f_4 = 1$, section 3) and some results obtained for $z = 5$, 6 will be quoted (section 4). Models will be compared with some actual structures and to simulation results.

The stable configuration is obtained by adding $z - 3$ sides at every z-vertex (Thompson 1917, ch 8, figure 158). Every added side is connected at least to one added side for $z > 4$ (figure 1(*c*, *d*)) and the associated graph is a connected graph without cycles, that is a tree (Berge 1970). The z *lattice* cells which meet at a z-vertex are numbered from 1 to z according to the following convention: a reference vertex is defined and the z cells meeting at this vertex are numbered. The numbering at every z-vertex belonging to the same family (same Schläfli sequence) is obtained by rotating the reference vertex and its z incoming sides in the positive sense by the smallest angle which brings both configurations in coincidence (figure 1(*c*)). This is possible as we allow, *if necessary*, defining angles and distances on the starting lattice. In that way, a clear meaning is attributed to a distribution of identical states on z-sites.

S_{kj} is the number of vertices of polygon number j at the considered lattice site. With a given added-side configuration and its z incoming sides, we associate all different circular permutations of the S_{kj} $(j = 1, \ldots, z)$ values among the z numbered positions. The total number of states is $Q(z)$, that is 14 states for $z = 6$, which are derived from the four configurations (figure 1(*d*)):

$$C_1 = \{122214\} \qquad C_2 = \{131313\} \qquad C_3 = \{123123\} \qquad C_4 = \{132132\}$$

The set of $Q(z)$ states is closed with respect to transformation T1 (figure 1(*a*)), that is any neighbour switching operation which may act on a given state ($(z - 3)$ possible operations) transforms it into a state of the set. Identity and neighbour switching transformations do not constitute a group (see the appendix). A configuration like C_3 becomes identical with C_4 by a circular permutation in the negative sense of rotation and both may be considered as one configuration. This is the implicit definition used

by Thompson (1917) who has considered the added-side configurations (ASC) but has not taken into account the various configurations of z sides which may be associated with a given ASC.

The sum

$$E_k = \sum_{j=1}^{z} S_{kj} = 3z - 6 \tag{2}$$

is independent of the configuration ($3z-6$ is simply obtained from the state S1, see the appendix). The sum E_k may also be calculated by considering z half great circles meeting at two poles on a sphere and two states among the $Q(z)$ states. We obtain equation (2) from the Euler-Poincaré characteristic: $2 = V - E + F$ with $2(z-2)$ vertices (V), E_k edges (E) and z faces (F). The number of states $Q(z)$ is 1, 2, 5, 14 for $z = 3$, 4, 5, 6 respectively. It increases exponentially with z, being 4.78×10^8 for $z = 20$. $Q(z)$ is given by a Catalan number (Knuth 1973, Viennot 1990, Le Caër 1991):

$$Q(z) = C_{2z-4}^{z-2}/(z-1). \tag{3}$$

In spite of the large number of states for large z values ($Q(z) \propto z^{-3/2}4^z$ when $z \to \infty$), a relation, giving the distribution $P_s(i, z)$ ($i = 1, 2, \ldots, z-2$) of the values of S_{kj} for a fixed j, can be derived ($P_s(i, \infty) = i/2^{i+1}$). $P_s(i, z)$ is useful for calculating $P(n)$ for a distribution of equiprobable and independent states on the sites, in particular in the case of spherical tessellations or of tessellations on surfaces topologically equivalent to a sphere. With two poles and z half great circles, we obtain for $z \to \infty$ and $n \geqslant 0$:

$$P(n) = n(n^2-1)/(2^n \times 24)$$

with $\langle n \rangle = 6$. This distribution may therefore be compared with $P(n)$ for planar cellular structures with $n \geqslant 2$. In fact, it differs little from the distribution of cell sides of the 2D Johnson-Mehl froth obtained for continuous nucleation with constant growth rate (Frost and Thompson 1987, Le Caër 1991).

The S_{kj} also allow defining the neighbours of a given cell. If we consider a cell of the starting lattice with n_L sides, its corresponding cell (n-cell) in the topological model will have two types of neighbours, as no neighbour switching takes place between different lattice sites: (i) n_L unconditional neighbours, (ii) $n - n_L$ conditional neighbours given by the S_{kj} values inside the considered lattice cell. At every vertex, $S_{kj} - 1$ lattice cells belong to that class of neighbours.

Neighbour switching between different sites may be performed by attributing a value to the bond connecting these two sites (for example 0 for no switching and -1 for switching).

3. The square lattice

For $z = 4$ on the square lattice or on a lattice topologically equivalent to a square lattice, we introduce a 'spin' $S = \pm\frac{1}{2}$ (figure 1(a)). Labelling as 1 the upper right corner of the central square in figure 1(b) and as 2 the upper left corner etc, the number of sides n ($4 \leqslant n \leqslant 8$) is given by

$$n = 6 + \sum_{j=1}^{4} (-1)^{j+1} S_j \tag{4}$$

while

$$nm(n,1) = 10 + 9n/2 - \frac{1}{2}\left\{\sum_{j=1}^{4} (-1)^j M_j^+\right\} + \sum_{j=1}^{4} S_j M_j^- \tag{5}$$

where $nm(n,1)$ is the total number of sides of the first-neighbour cells of a given central n-cell. The average over all configurations of spins, for a fixed n, is $nm_n(1) = \overline{nm(n,1)}$. Both $M_j^{\pm}$ are given by an algebraic sum of three spins at every corner of the outer square (figure 1(b)) which includes the nine interior squares. The relative position of S_j and M_j is also shown in figure 1(b). $M_j^{\pm}$ is the sum of the corner spin plus or minus the sum of its two neighbour spins, one per side of the outer square. The last sum in equation (5) is due to conditional neighbours which are responsible for the presence of pair correlations in that term.

An exact but lengthy expression has also been calculated for $s(n)m(n,2)$ where $s(n)$ is the number of second-neighbour cells of a central n-cell. If the spins are independently distributed on every site with a probability p for $S = \frac{1}{2}$, a symmetric $P(n)$ distribution (table 1) with $\mu_2 = 4p(1-p)$ is obtained.

The average, for a fixed n, yields:

$$m_n(1) = p + 4 + (13 - 6p)/n + (1-2p)A_d(n)/n \tag{6}$$

where $A_d(n)$ is given in table 1 with, as expected, $\langle nm_n(1)\rangle = \mu_2 + 36$. Moreover, $s_n = \overline{s(n)}$:

$$s_n = n(m_n(1) - 4) \tag{7}$$

and

$$m_n(2) = \overline{s(n)m(n,2)}/s_n = \{6 + 3\mu_2 + n(5m_n(1) - 19 - \mu_2/4)\}/\{n(m_n(1) - 4)\}. \tag{8}$$

For $p = \frac{1}{2}$, the standard deviation of the distribution of $m(n,1)$ as a function of n is

$$sd_m(n) = (12 - n)^{1/2}/(2n). \tag{9}$$

This simple model already grasps many characteristic features of cellular structures.

With the present rule, the Aboav–Weaire law (equations (1) and (6)) is only exact for $p = \frac{1}{2}$ with $a = 1.5$ but is otherwise a very good approximation (relative error less than ~2% for p as small as 0.1) with a least-square value a_L ($4 \leqslant n \leqslant 8$), given by (10) which may be useful for comparison with experimental results ($1.5 \leqslant a_L \leqslant 1.777$):

$$a_L = 1.5 + 3M^2\{(1225 + 1481M^2)/(1 + M^2)\}/14618 \qquad M = 2p - 1 \tag{10}$$

The weak dependence of $m_n(2)$ on n (table 1) is also observed in computer simulations of the coarsening of random cellular systems (Nakashima *et al* 1989).

Table 1. Distribution of the number of cell sides $P(n)$, $A_d(n)$ term in equation (6), and $m_n(2)$ for $p = \frac{1}{2}$ (equation (8)) for $z = 4$ on a square lattice.

n	4	5	6	7	8
$P(n)$	$p^2(1-p)^2$	$2p(1-p)^3 + 2p^3(1-p)$	$p^4 + (1-p)^4 + 4p^2(1-p)^2$	$2p(1-p)^3 + 2p^3(1-p)$	$p^2(1-p)^2$
$A_d(n)$	-1	$\dfrac{-(1-p)^2}{[p^2 + (1-p)^2]}$	$\dfrac{p^4 - (1-p)^4}{P(6)}$	$\dfrac{p^2}{[p^2 + (1-p)^2]}$	1
$m_n(2)$ $(p = 0.5)$	6	6.02	6.0385	6.0555	6.0714

The standard deviation $sd_m(n)$ has been observed to be very well described by a linear dependence on $m_n(1)$ for the random Voronoi froth as well as for the Voronoi tessellation generated from eigenvalues of complex random matrices with respective slopes of 0.241 and 0.162 (Le Caër and Ho 1990). To a good approximation (mean absolute deviation 6×10^{-3}), $sd_m(n)$ (equation (9)) is given by

$$sd_m(n) = 0.1824 m_n(1) - 0.922. \tag{11}$$

Finally, as some experimental or simulation results also show symmetric distributions $P(n)$ with negligible contributions for $n<4$ or $n>8$, we have compared their $P(n)$ with the calculated ones. The agreement is, to our surprise, satisfactory in a wide p range (table 2). It will however be necessary to introduce switchings between neighbouring sites or (and) face disappearances in order to create some cells with $n=3$ or $n\geqslant 9$ and to allow varying $m_4(1)$ and $m_8(1)$. We will also have to confirm that the correlations between cells are correctly represented by the model.

This is the case for the hard disk simulation (table 2, Fraser 1991 and to be published). Simulations of dense 2D liquids, with particles interacting through a truncated Lennard-Jones pair potential which is short-ranged and purely repulsive, have been performed by Glaser and Clark (1990). Besides $P(n)$ for Voronoi tessellations (table 2), they have calculated the distribution of disclination charges n_D (inset of figure 1c of their paper.) Some bonds of the Delaunay tessellation are removed in order to tile the plane with quadrilaterals and triangles. The resulting structure is compared with the Collins tiling model composed of squares and equilateral triangles. A charge $n_D=0$ is attributed to the four allowed local configurations in the latter model. The charges $n_D\neq 0$ characterize deviations from this ideal tiling. It is striking

Table 2. Comparison between experimental or simulated distributions and calculated distributions (in brackets, table 1) for $z=4$, here on a lattice topologically equivalent to a square lattice: (i) $P_{exp}(n)$ for a cellular tissue in a human amnion (Lewis 1931): 1000 cells, $P_{exp}(3)=0.004$ and $P_{exp}(9)=0.007$ ($P_{model}(3)=P_{model}(9)=0$). (ii) $P_{exp}(n)$ for the epidermal epithelium of the cucumber (Lewis 1928) 1000 cells, $P_{exp}(9)=0.001$ ($P_{model}(9)=0$). (iii) Cellular arrays obtained during upward solidification of Pb-30wt% Tl: a typical distribution (Nguyen Thi *et al* 1990). (iv) Monte Carlo simulation for hard disk models in 2D: distribution $P_{sim}(n)$ for the associated Voronoi tessellation and, for example, a pressure of $8.05kT\times d^{-2}$ (d hard-disk diameter) (figure 6 of Fraser *et al* 1990 and personal communication). (v) Monte Carlo simulation for a 2D liquid with 896 particles and a truncated Lennard-Jones (TLJ) pair potential: $P_{sim}(n)$ (Voronoi tessellation) and disclination charge distribution $P_{sim}(n_D)$ for a number density of 0.83 (Glaser and Clark 1990).

n	4	5	6	7	8
Human amnion ($p=0.645$)	0.054 (0.052)	0.248 (0.248)	0.397 (0.399)	0.241 (0.248)	0.049 (0.052)
Cucumber ($p=0.763$)	0.020 (0.033)	0.251 (0.231)	0.474 (0.473)	0.224 (0.231)	0.030 (0.033)
Pb-Tl alloys ($p=0.827$)	0.02 (0.020)	0.21 (0.205)	0.55 (0.55)	0.19 (0.205)	0.03 (0.020)
hard disks ($p=0.907$)	0.001 (0.007)	0.146 (0.140)	0.709 (0.706)	0.141 (0.140)	0.003 (0.007)
2D liquid, TLJ ($p=0.933$)	0.000 (0.004)	0.114 (0.110)	0.775 (0.773)	0.109 (0.110)	0.002 (0.004)
2D liquid, $n=6+n_D$ ($p_D=0.828$)	0.010 (0.020)	0.218 (0.204)	0.554 (0.551)	0.200 (0.204)	0.019 (0.020)

to observe that the distribution of n_D looks like $P(n)$ if we define $n = 6 + n_D$, with a probability p_D which differs from p (table 2). For number densities of 0.70 and 0.85, we also obtain $\text{Prob}(\{|n_D| \leq 1) = 0.905$ and 0.975 (with $p_D = 0.679$ and 0.873) as compared with simulation values of 0.884 and 0.980 respectively.

In conclusion, it seems that the $z = 4$ models may serve as a zeroth-order approximation of the topology of some actual structures. The question of the connections between these models and natural structures is therefore raised. Our structures are homogeneous and by construction they satisfy the constraint of space-filling and the Euler's relation $\langle n \rangle = 6$. Randomness is also present but these structures are not in statistical equilibrium as defined by Rivier (1985, 1986) in his statistical mechanics theory of random tissues: our structures are not invariant under structural transformations such as T1 and T2 (introduction) as both will for example create triangles which do not exist for $z = 4$. As any lattice topologically equivalent to a square lattice gives the same result as above, we suggest that it is the existence of two-state entities which has some connection with the actual systems but we still ignore the deep meaning of the previous observations. In a very recent paper, Jones (1990) emphasizes that 'although it is mysterious, the evidence for a connection between knot theory and statistical mechanics is substantial'. It is not obvious that this remark is far from our subject as topology is the relevant geometry for cellular structures (Rivier 1986) and also as striking similarities exist between the two states of figure 1(*a*) and the two states of the Kauffman model (Jones 1990) which determine how the crossings in a link will be eliminated.

Topological models may also be associated with distributions of spins given by Ising models. The side-number distribution $P(n)$ can, for example, be exactly determined for a ferromagnetic Ising model on a square lattice having only nearest-neighbour couplings. Equation (4) is used to calculate the moments $\mu_k = \langle (n-6)^k \rangle$. By symmetry, all odd-moments are zero and $P(n)$ is therefore symmetric with respect to $n = 6$. As the even moments only depend on four spins located on the vertices of the central square of figure 1(*b*), they may all be expressed as a function of the two-pair correlation coefficients and the quartet correlation coefficient which can be defined on that square:

$$x_1 = 4\langle S_j S_{j+1} \rangle \qquad x_2 = 4\langle S_j S_{j+2} \rangle \qquad x_{12} = 16\langle S_1 S_2 S_3 S_4 \rangle \tag{12}$$

where j has any value between 1 and 4. These correlation coefficients have been determined exactly at all temperatures T/T_c (see for example Khatun *et al* 1990 and references therein). With $d = 2x_1 - x_2$, equations (4) and (12) yield:

$$\begin{aligned}
&\mu_2 = 1 - d \qquad \mu_4 = \tfrac{5}{2} + 3x_{12}/2 - 4d \\
&P(4) = P(8) = (1 + x_{12})/16 - d/8 = P_r(4) + G_{12}/16 - G_d/8 \\
&P(5) = P(7) = (1 - x_{12})/4 = P_r(5) - G_{12}/4 \\
&P(6) = 3(1 + x_{12})/8 + d/4 = P_r(6) + 3G_{12}/8 + G_d/4
\end{aligned} \tag{13}$$

where $G_{12} = x_{12} - M^4$, $G_d = d - M^2$ and M is the magnetization. As expected, $P(6)$ is increased (for $T/T_c \neq 0, \infty$) (see figures 3-5 of Khatun *et al* for the temperature dependence of the xs) with respect to $P(6)$ in a distribution of non-interacting spins with the same magnetization, that is $p = (1 + M)/2$ in $P_r(n) = P(n)$ of table 1. On the contrary all the other $P(n)$s, $n \neq 6$, are decreased.

The model associated with the Kagomé net ($z = 4$), which is a quasi-regular tessellation (Coxeter 1973, Frank and Kasper 1958) built from hexagons and triangles, has also been studied. According to the value of p, bimodal $P(n)$ distributions, coming from the two different populations of polygons, are calculated (Le Caër 1991). For

$z=4$, the chosen rule is the neighbour switching T1 transformation which is simply described by spin flipping (figure 1(a)). The spin description must not be pushed too far as a cellular structure may be described differently if the starting lattice is a square ($P(6)=1$, ferromagnetic configuration at 0 K), a Kagomé net ($n=6$ for $p=0$ but $n=3$ and 12 for $p=1$), a triangular lattice or any other lattice.

Triangle creation can be included in the rule and gives rise to an increased number of states. The distribution $P(n)$ calculated for a random creation of triangles on the vertices of the cellular structure associated with a square lattice will be published later. The use of bonds between lattice sites (end of section 2) may lead to significant cell annihilation if the density of bonds with non-zero values is large enough and constitute an interesting extension of the method for square lattices.

4. Some results for $z>4$

For $z>4$, calculations are not as simple as for $z=4$ but raise no major difficulties. In particular numerical values may be precisely obtained with a microcomputer. For any value of z, the distribution $P(n)$ can also be exactly determined in the case of equiprobable ($p_i=1/Q(z)$) and independent states on every lattice site (Le Caër 1991). Many tilings which are worth being investigated by the present method are described by Grünbaum and Shephard (1987). Calculations of the distributions $P(n)$ and of $m_n(1)$ have been performed for $z=5$ and the lattice of figure 1(c), which is topologically equivalent to a basic net occurring in complex alloys structures (Frank and Kasper 1958, Sadoc and Mosseri 1982), and for $z=6$ on the triangular lattice (figure 1(d)). In both cases, n goes from 3 to 12 ($4(z-2)$ for $z=5$, $3(z-2)$ for $z=6$). Figures 2 and 3 show the results for $z=5$, $p_i=0.2$, $i=1,\ldots,5$ ($\mu_2=2.5714$, $a=1.198$) and for $z=6$, $p_i=\frac{1}{14}$, $i=1,\ldots,14$ ($\mu_2=2.5867$, $a=0.974$). Three conclusions may be drawn.

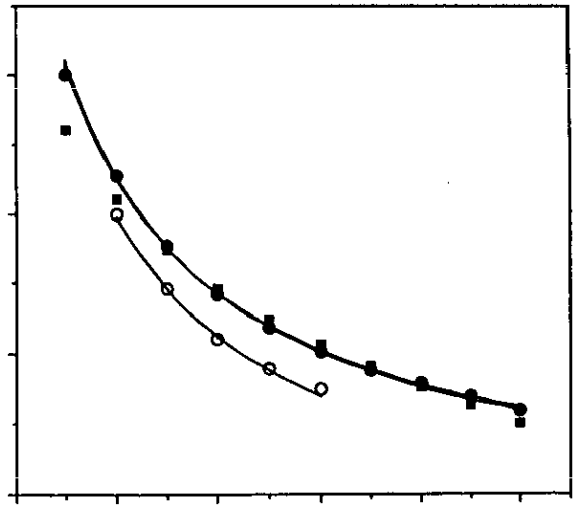

Figure 2. Mean number of sides $m_n(1)$ of n-cells as a function of n (open circles $z=4$, $p=0.25$, square lattice, full circles $z=5$, $p_i=0.2$, lattice of figure 1(c), full squares $z=6$, $p_i=\frac{1}{14}$, triangular lattice). Full curves correspond to the best fits with the Aboav-Weaire law (equation (1)) with $a=1.565$, 1.198 for $z=4$, 5 respectively.

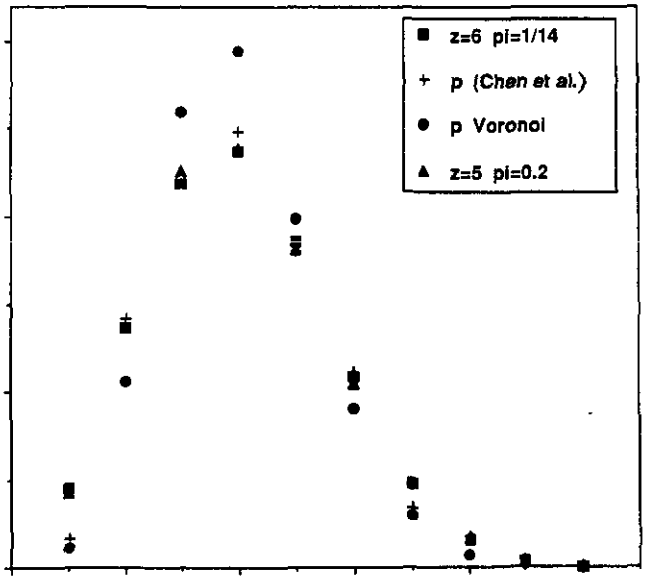

Figure 3. Distribution $P(n)$ of the number n of cell sides for $z = 5$, 6 (lattices of figure 1(*c*), (*d*)), for a random Voronoi tessellation (Le Caër and Ho 1990) and for the domain structure in thin films of glassy As_2Se_3 (Chen *et al* 1984).

(i) The Aboav–Weaire law is not rigorous for the chosen rule but is again a very good approximation in many cases. For $z = 6$, strong deviations from equation (1) occur, mainly for $n = 3$ and for $n > 8$, as also seen for soap froths and for Voronoi tessellations (Aboav 1980, Le Caër and Ho 1990).

(ii) The values of a (figure 2) are in some cases almost exactly 1.2 which are also typically found in natural structures (Aboav 1980). Similar values are still calculated for the case of non-equiprobable states.

(iii) The $P(n)$ distributions are similar for $z = 5$ and $z = 6$. They are realistic as shown in figure 3 where they are compared with actual distributions. However, $P(n)$ for equiprobable and independent states does not account for the observed values in 2D soap froths (Stavans and Glazier 1989) as, for example, $P(5)$ and $P(6)$ are too small.

5. Conclusions

The method that we have described is useful for creating models of cellular structures and for studying their topological properties. Like the method of Sadoc for amorphous structures (see Sadoc and Mosseri 1982), it associates a disordered system with an ordered one. The next step will be to include cell creation and cell annihilation in the rule while keeping the advantages of working on lattices. Both topological transformations T1 and T2 are needed to reach statistical equilibrium (Rivier 1986) which may be worth investigating with the present method. Cellular structures may also be associated with Ising models ($z = 4$), Potts models ($z > 4$) or cellular automata. Tessellations in curved spaces (Sadoc and Mosseri 1982) constitute obvious extensions of the method and preliminary results have been obtained. Finally, it would be interesting to try to define side lengths and angles in the cellular structures.

Acknowledgments

I thank R Delannay, J M Dubois, D P Fraser, T Liebling, A Mocellin, F Montoya and F Righetti for useful discussions.

Appendix

The neighbour switching transformations are represented here by one-dimensional matrices T with z elements. If the matrix elements ($z-4$ zeros, two 1 and two -1) are written on a circle, the $+1$ and -1 alternate and possibly separated by groups of zeros. We adopt the following notation: T^{e}_{ijkl} means $T(i)=+e$, $T(j)=-e$, $T(k)=+e$ and $T(l)=-e$, with $e=\pm 1$.

The result of the neighbour switching transformation T^{e}_{ijkl} applied to a state S_k is simply obtained by adding the elements of both matrices. The transformation is, however, impossible if the resulting matrix contains a zero or a value of $(z-1)$ or two successive 1 or less than two 1 (any added-side configuration has at least two ends). Any T^{e}_{ijkl} cannot act on any state and the product of two operations cannot be always defined. For example, the neighbour switching $T^{+}_{1236}=(1-1100-1)$ $(z=6)$ transforms the state (122214) (configuration C_1, section 2) into the state (213213) which belongs to configuration C_4 but T^{+}_{1236} cannot act on (412221) to give (503220). T^{+}_{2356} cannot operate on (213213) to give (222222) (there are no added-side cycles). For a given z, all states may be generated by applying the neighbour switching transformations to a $S_1=(1, z-2, 1, 2, 2, \ldots, 2)$ state and to the states derived from S_1 etc, until a closed set is obtained.

References

Aboav D A 1970 *Metallography* **3** 383–90
—— 1980 *Metallography* **13** 43–58
Berge C 1970 *Graphes et Hypergraphes* (Paris: Dunod)
Blanc M and Mocellin A 1979 *Acta Metall.* **27** 1231–7
Chen C H, Philips J C, Bridenbaugh P M and Aboav D A 1984 *J. Non-crystalline Solids* **65** 1–28
Coles P 1990 *Nature* **346** 446–7
Coxeter H S M 1973 *Regular Polytopes* (New York: Dover)
Fortes M A and Andrade P N 1989 *J. Physique* **50** 717–24
Frank F C and Kasper J S 1958 *Acta Cryst.* **11** 184–90
Fraser D P 1991 *Materials Characterization* in the press
Fraser D P, Zuckermann M J and Mouritsen O G 1990 *Phys. Rev.* A **42** 3186–95
Frost H J and Thompson C V 1987 *Acta Metall.* **35** 529–40
Glaser M A and Clark N A 1990 *Phys. Rev.* A **41** 4585–8
Grünbaum B and Shephard G C 1987 *Tilings and Patterns* (San Francisco: Freeman)
Jones V F R 1990 *Scientific American* **263** 98–103
Khatun M, Barry J H and Tanaka T 1990 *Phys. Rev.* B **42** 4398–405
Knuth D E 1973 *The Art of Computer Programming* vol 1, 2nd edn (Reading, MA: Addison-Wesley)
Le Caër 1991 *in preparation*
Le Caër G and Ho J S 1990 *J. Phys. A: Math Gen.* **23** 3279–95
Lewis F T 1928 *The Anatomical Record* **38** 341–76
Kewis F T 1931 *The Anatomical Record* **50** 235–65
Marians C S and Burdett J K 1990 *J. Non-Cryst. Solids* **124** 1–21
Meijering J L 1953 *Philips Res. Rep.* **8** 270–90
Nakashima K, Nagai T and Kawasaki K 1990 *J. Stat. Phys.* **57** 759–87

Nguyen Thi H, Billia B and Capella L 1990 *J. Physique* **51** 625–37
Rivier N 1985 *Phil. Mag.* B **52** 795–819
—— 1986 *Physica* **23D** 129–37
Sadoc J F and Mosseri R 1982 *Phil. Mag.* B **45** 467–83
Smalley I J 1966 *Geol. Mag.* **103** 110–4
Stavans J and Glazier J A 1989 *Phys. Rev. Lett.* **62** 1318–21
Thompson D' A W 1917 *On Growth and Form* (Cambridge: Cambridge University Press)
Viennot X G 1990 *Trees everywhere: Proc. CAAP'90, Copenhagen May 1990, Lecture Notes in Computer Science* in press
Weaire D 1974 *Metallography* **7** 157–60
—— 1983 *Topological Disorder in Condensed Matter* ed F Yonezawa and T Ninomiya (Berlin: Springer) pp 51–9
Weaire D and Rivier N 1984 *Contemp. Phys.* **25** 59–99